



# Chronic social defeat stress-induced depression reduces BCG efficacy by promoting regulatory T-cell levels in mice

Rohit Tyagi<sup>1</sup>, Xi Chen<sup>1</sup>, Atika Dhar<sup>2</sup>, Bing Yang<sup>1</sup>, Wei Zhou<sup>1</sup>, Aikebaier Reheman<sup>1,3</sup>, Yingying Lei<sup>1\*</sup>  and Gang Cao<sup>1,4\*</sup>

## Abstract

Despite the initial successes of the Bacillus Calmette-Guerin (BCG) vaccine in children, its efficacy against tuberculosis is highly variable. There is a lack of understanding about how mental conditions influence BCG vaccination. Here, we used the chronic social defeat stress (CSDS) model to explore the effects of depression on BCG vaccination efficacy. We observed higher lung and spleen bacterial loads and a lower organ index in depressed compared to BCG mice. Meanwhile, a relatively lower T cell protective efficacy was observed in both compared to control and BCG mice via a mycobacterium growth inhibition assay (MGIA). Cytokine expression of IL-12p40, IL-1 $\beta$ , IL-17, TNF- $\alpha$  and IFN- $\gamma$  was reduced, whereas the expression of IL-10 and IL-5 was increased in the spleen of both compared to BCG mice. Moreover, the proportions of CD4<sup>+</sup>IFN- $\gamma$ <sup>+</sup>, CD8<sup>+</sup>IFN- $\gamma$ <sup>+</sup> T lymphocytes and CD4<sup>+</sup> effector/central memory T cells were reduced in the splenocytes of the depressed BCG mice. Depression promotes CD4<sup>+</sup> regulatory T cells (Treg) and myeloid-derived suppressor cell (MDSC) generation in depressed mice, contributing to the reduced pro-inflammatory immune response upon BCG vaccination. This study provides insight into the decreased protective immunity by BCG vaccination attributable to depression in mice.

**Keywords** BCG, Vaccine efficacy, Treg, Immune suppression, Depression

## Introduction

The *Mycobacterium tuberculosis* (*M. tuberculosis*) complex shares high genetic homology, varying pathogenicity and broad infection hosts, including humans,

domestic livestock, wild animals and non-human primates (H. Zhang et al. 2022). *Mycobacterium bovis* is a cattle pathogen with a zoonotic risk to humans (Romha et al. 2018). The number of active tuberculosis (TB) patients increased from 10.1 million in 2020 to 10.6 million in 2021, together with 1.6 million deaths (Bagchi, 2023) and nearly \$3 billion in annual losses in the livestock industry (Gong et al. 2021). Although the clinical differentiation of infection by either *M. tuberculosis* or *M. bovis* is not possible, up to 10% of human tuberculosis cases are associated with *M. bovis* in some countries (Khan et al. 2019). Bacillus Calmette-Guerin (BCG) remains the only World Health Organization (WHO)-recognized vaccine candidate in children (Moliva et al. 2017) and facilitates the control of bovine tuberculosis (Williams et al. 2022; Buddle et al. 2016). However,

\*Correspondence:

Yingying Lei

leiyingying@webmail.hzau.edu.cn

Gang Cao

gcao@mail.hzau.edu.cn

<sup>1</sup> National Key Laboratory of Agricultural Microbiology, College of Veterinary Medicine, Huazhong Agricultural University, Wuhan 430070, China

<sup>2</sup> National Institute of Immunology, New Delhi 110067, India

<sup>3</sup> College of Animal Science and Technology, Tarim University, Alar 843300, China

<sup>4</sup> Bio-Medical Center, Huazhong Agricultural University, Wuhan 430070, China



© The Author(s) 2023. **Open Access** This article is licensed under a Creative Commons Attribution 4.0 International License, which permits use, sharing, adaptation, distribution and reproduction in any medium or format, as long as you give appropriate credit to the original author(s) and the source, provide a link to the Creative Commons licence, and indicate if changes were made. The images or other third party material in this article are included in the article's Creative Commons licence, unless indicated otherwise in a credit line to the material. If material is not included in the article's Creative Commons licence and your intended use is not permitted by statutory regulation or exceeds the permitted use, you will need to obtain permission directly from the copyright holder. To view a copy of this licence, visit <http://creativecommons.org/licenses/by/4.0/>. The Creative Commons Public Domain Dedication waiver (<http://creativecommons.org/publicdomain/zero/1.0/>) applies to the data made available in this article, unless otherwise stated in a credit line to the data.

its protective efficacy is still lower in high infection areas that vary from 0–80% and gradually wanes after adolescence (Abubakar et al., 2013; Roy et al., 2014). The role of depression in decreasing BCG-mediated prophylaxis is unknown and is crucial for innate immunity activation and subsequent development of adaptive immunity.

Unfortunately, the lack of investigation around vaccine failure due to mental well-being and mood-related disorders persists (Moliva et al. 2017). The WHO designated depression as the most prevalent psychiatric disorder and disabling medical condition, and by 2030, it had been proposed that depression would be the biggest contributor to disease burden (Bains and Abdijadid, 2023). Chronic stress reduces immune responses, including declining leukocyte transfer, weakening neutrophil phagocytosis, and decreasing the frequency of lymphocytes (Seiler et al. 2020). Social defeat mimics the childhood adversities, traumas and bullying that generate mood-related disorders such as anxiety, depression and schizophrenia events and substantially influence brain development in adults (Waters and Gould, 2022). Interestingly, behavioral alterations in mice due to social defeat stress, such as decreased social interaction or lack of gratification, illustrate human depression (Hales et al. 2014). Mice are

considered in our study because they mimic the immune response generated against *M. tuberculosis* infection in other larger animals (Singh and Gupta, 2018).

In the present study, we analyzed the difference in the BCG vaccine response in depressed mice using the chronic social defeat stress (CSDS) model. In both depressed and depressed BCG mice, the mRNA expression of the cytokines IFN- $\gamma$ , IL-12p40, IL-1 $\beta$ , IL-17, and TNF- $\alpha$  decreased significantly, while that of IL-5 and IL-10 increased. Furthermore, CD4<sup>+</sup>IFN- $\gamma$ <sup>+</sup>, CD8<sup>+</sup>IFN- $\gamma$ <sup>+</sup> and CD4<sup>+</sup> memory T cells decrease. While, the CD4<sup>+</sup> Treg and MDSC cells increase in both depressed and depressed BCG mice. This study provides a better understanding of how depression in the host affects the immune-modulatory response to BCG vaccination.

## Results

### Chronic Social Defeat Stress (CSDS) induces mood-related depressive behavior in mice

To investigate the effects of depression on BCG vaccination, we generated a chronic social defeat stress mouse model. As shown in Fig. 1A, four groups of C57BL/6 male mice (control, BCG, depressed, and depressed BCG)

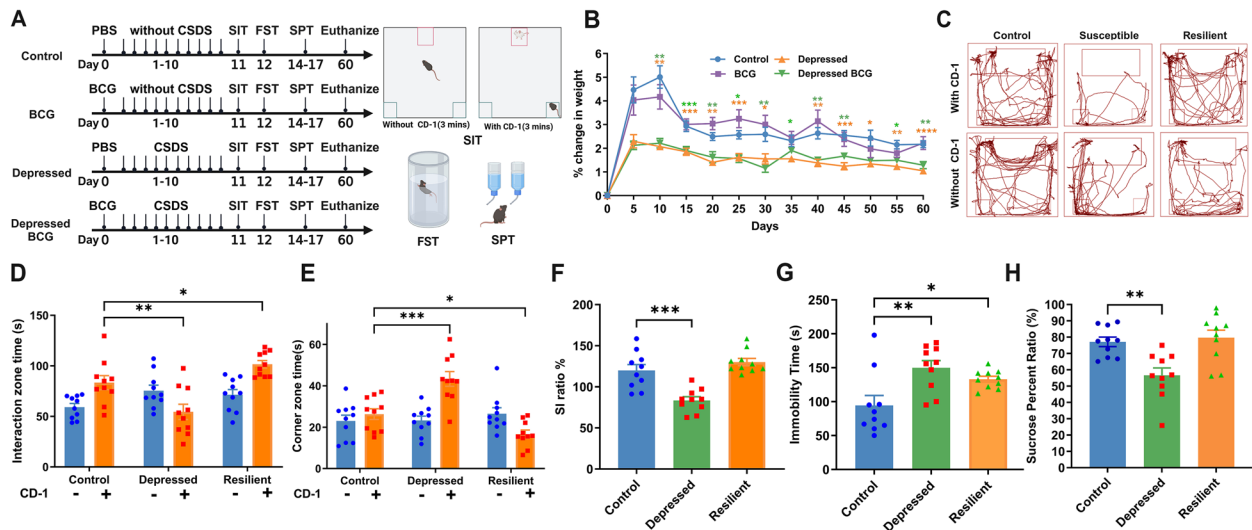


**Fig. 1** Chronic social defeat stress (CSDS) induces depressive behavior in mice. **A** Schematic diagram of the experimental design representing all four groups of mice. While, in **C-H** two separate group namely (susceptible and resilient mice) generated according to their performance in the behavior tests with respect to the naive control group. C56BL/6 mice were subjected to CSDS-induced depression and assessed by the social interaction test (SIT), swimming test (FST) and sucrose preference test (SPT). **B** The figure represents the percent change in the weight of each mouse group recorded every 5 days. (**C-H**) Behavior tests contain three groups (control, depressed and resilient). **C** Representative movement map of SIT information for control, susceptible and resilient mice generated with PANLAB software. **D-E** Statistical analysis of movement parameters in the SIT by calculating the time spent by each mouse in the interaction or corner zones after undergoing the CSDS procedure. **F** Social interaction (SI) ratio % was calculated by using the formula described in the methods section to differentiate each mouse into depressed or resilient by analyzing the total time spent in each zone. **G** The FST results were analyzed by observing the immobility time of each mouse from the total recorded swimming duration of 4 min. **H** The sucrose percent ratio was calculated according to the formula added in the material and method by performing the SPT. \*,  $p \leq 0.05$ ; \*\*,  $p \leq 0.01$ ; \*\*\*,  $p \leq 0.001$ ; \*\*\*\*,  $p \leq 0.0001$  (two-way ANOVA). Data are representative of three independent experiments with three biological replicates (mean  $\pm$  SEM)

were subjected to BCG immunization and chronic social defeat stress. Body weight was significantly reduced in depressed and depressed BCG mice in comparison to the control and BCG mice (Fig. 1B). The social interaction test (SIT) was conducted to assess depressive behavior. Our results showed that when depressed mice stayed with CD-1 mice, they spent significantly more time in the corner zones and less time in the interaction zone than control mice. Resilient mice interact more with CD-1 mice, leading to increased duration within the interaction zone and lower duration in the corner time in contrast with the control mice (Fig. 1C-E). SI % (social interaction) ratio score depicting the susceptible and resilient phenotypes. A score less than 100% was considered susceptible, while a score of more than 100% was considered resilient (Fig. 1F). The forced swimming results showed that the depressed mice lacked the desire to swim and spent a longer time immobile than the control mice (Fig. 1G). The sucrose preference test (SPT) results showed that total liquid intake was significantly reduced in depressed mice compared to control mice (Fig. 1H). Our data demonstrate the existence and evaluation of the depressive mood-related behavior generated in socially defeated mice.

#### Reduced organ index, higher bacterial load, and lower in vitro BCG efficacy in depressed mice

Next, we analyzed the organ index and bacterial load in all the subjects. We found a decreased organ index of both the spleens and the lungs in depressed BCG mice (Fig. 2A, B). H&E staining of the mouse lungs showed more inflammatory cell infiltration in BCG-infected mice than in depressed BCG subjects. This suggests a lowering BCG response in the lungs of depressed BCG mice (Fig. 2C). The bacterial load was higher in depressed BCG mice than in BCG mice (Fig. 2D, E). The MGIA assay was used to evaluate the immune efficacy of BCG vaccination within different mouse groups (Pepponi et al. 2017) (Fig. 2F). A clear difference in the action of effector T cell can be seen in their respective groups, showing their distinct efficiency in clearing intracellular mycobacteria (Fig. 2G). We found that the clearance of intracellular mycobacteria within target BMDM cells by effector T cells after BCG vaccination declined significantly in depressed mice, while lower protection by effector T cells was detected in the depressed BCG group. (Fig. 2H). A clear indication that the efficiency of effector T cells was decreased due to depression (Fig. 2H). Together, these data demonstrate that the physiological changes in depressed mice lead to dwindling BCG vaccination efficacy and an immune response toward mycobacterium infection.

#### Depression in mice leads to a reduced proinflammatory response after BCG immunization

To investigate the causes of decreased immunity in depressed subjects, we analyzed the expression of the cytokines IFN- $\gamma$ , IL-12p40, IL-1 $\beta$  and TNF- $\alpha$  in the spleen. As shown in Fig. 3A-D, the BCG-immunized mice had a higher fold change in IFN- $\gamma$ , IL-12p40, IL-1 $\beta$  and TNF- $\alpha$  than the control mice. Interestingly, the BCG-immunized depressed mice expressed significantly lower IFN- $\gamma$ , IL-12p40, IL-1 $\beta$  and TNF- $\alpha$  in comparison to the BCG-immunized mice.

Both CD4<sup>+</sup> and CD8<sup>+</sup> T cells are capable of responding to *M. tuberculosis* antigens by activating both humoral and cellular immunity (Simmons et al. 2018). Thus, we quantified both CD4<sup>+</sup> and CD8<sup>+</sup> T cells by using flow cytometry and found that both CD4<sup>+</sup> and CD8<sup>+</sup> T cells were significantly increased in BCG mice. However, it was lower down in the depressed BCG mice compared with the BCG mice (Fig. 3E-G). Furthermore, we analyzed IFN- $\gamma$ -producing T cells in response to the *M. tuberculosis* antigen and found a reduction in IFN- $\gamma$  production by CD4<sup>+</sup> and CD8<sup>+</sup> T cells in depressed mice (Fig. 3H-K). As memory CD4<sup>+</sup> T cells are important for providing long-term immunity after immunization (Henaio-Tamayo et al. 2010), we assessed the ratio of these cells. CD4<sup>+</sup> and CD8<sup>+</sup> T cells with the phenotype of naïve (naïve, CD25<sup>-</sup>CD44<sup>-</sup>CD62L<sup>+</sup>), effector memory (effector memory, CD25<sup>-</sup>CD44<sup>+</sup>CD62L<sup>-</sup>), and central memory (central memory, CD25<sup>-</sup>CD44<sup>+</sup>CD62L<sup>+</sup>) cells were gated (Fig. 3L and Supplementary Fig. 2A). A lower ratio of central and effector memory CD4<sup>+</sup> T cells in the spleen of naïve and BCG-immunized mice was observed in comparison to naïve/immunized mice (Fig. 3M-N). The percentages of both effector and central memory CD8<sup>+</sup> T cells were lower without a significant difference in the depressed BCG group of mice (Supplementary Fig. 2B, C). Thus, CD4<sup>+</sup> memory T cells have greater stature (Yang et al. 2018). Together, these data demonstrate dwindling protective immunity via lower localized proinflammatory and cellular response generation in depressed BCG mice.

#### Immune-suppressive cytokines and Tregs amplified in the spleens of depressed BCG mice

We measured the mRNA expression of IL-10, IL-17, and IL-5 in the total splenocytes of the mice and found that the BCG depressed mice had higher expression of IL-10 and IL-5 than the BCG group. IL-17 production in depressed subjects showed a downward response (Fig. 4A-C). Such alterations in IL-10 and IL-17 could further contribute to poorer bacterial clearance in depressed mice.

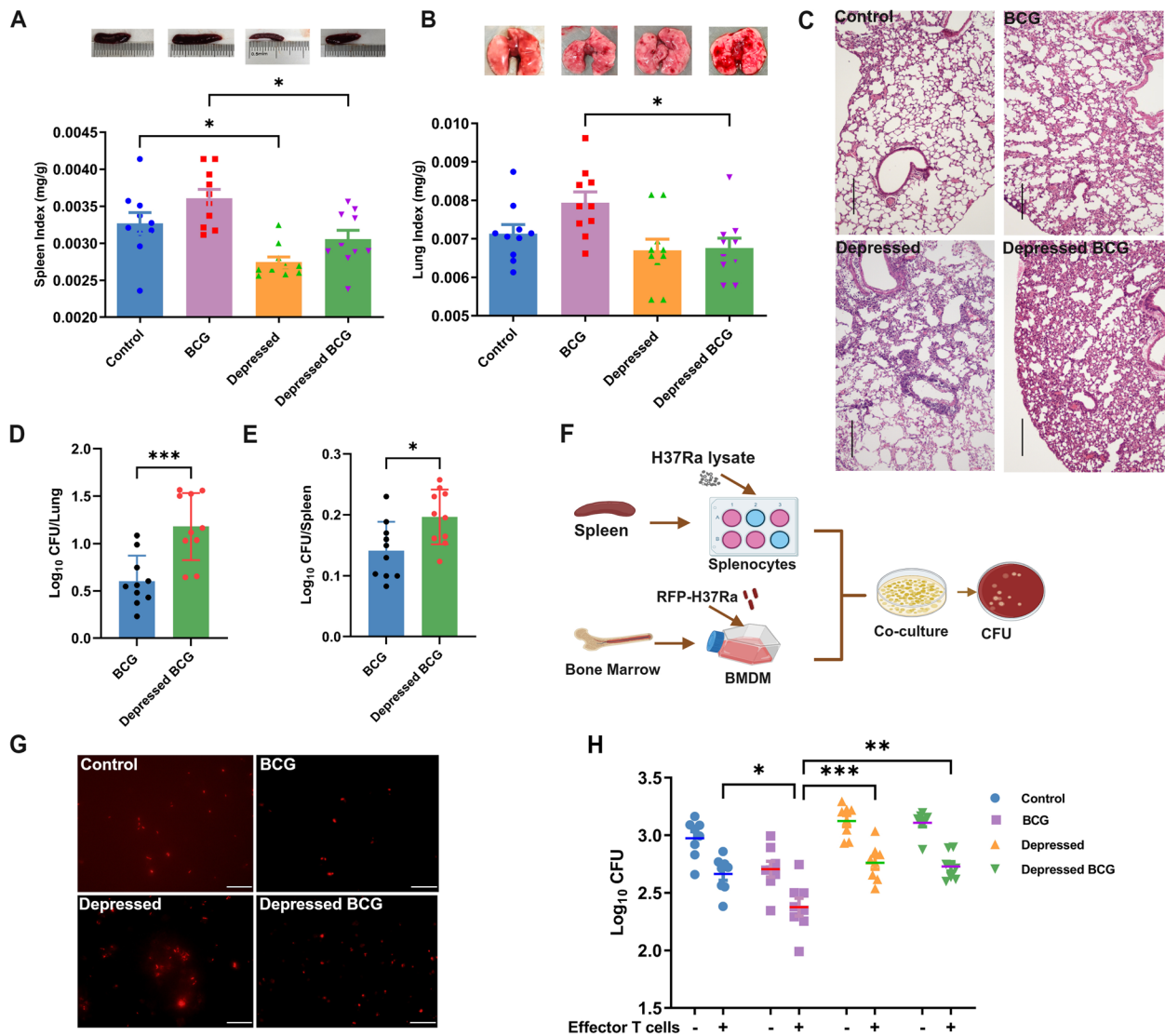


**Fig. 2** Evaluating BCG efficacy by organ pathology and Mycobacterium growth inhibition assay (MGIA) assay (**A, B**) Spleen and lung organ index calculated by taking the ratio of the organ weight to total weight of each mouse. Illustrated pictures from each group showing lung and spleen taken for weight and organ physiological studies. **C** H&E staining of lung sections, 200x magnification (scale bar: 200  $\mu$ m). **D, E** CFU in the lung and spleen of the BCG infected groups. **F** Pictorial diagram to represent the MGIA procedure as discussed in the methods section. **G** The visualization of effector T cells in action against intracellular RFP-H37Ra in BMDM cells using fluorescence microscopy in all four groups of mice, 100x magnification (Scale bar:100  $\mu$ m). **H** Viable intracellular RFP-H37Ra inside BMDMs with and without coculture of effector T cells was evaluated by counting CFUs in all four groups of mice. \*,  $p \leq 0.05$ ; \*\*,  $p \leq 0.01$ ; \*\*\*,  $p \leq 0.001$ ; \*\*\*\*,  $p \leq 0.0001$ . Statistical analysis in **A** and **B** was calculated by one-way ANOVA and **H** by two-way ANOVA, while **D** and **E** were calculated by unpaired t test. Data are representative of three independent experiments with three biological replicates (mean  $\pm$  SEM)

To further understand the role of different immune cell subsets with known suppressive functions in the observed reduction in BCG responses in depressed mice, we assessed the percentage of Tregs and MDSCs among the total splenocytes of the four groups of mice. Our results showed that the total number of Tregs was increased in the spleens of depressed mice and

BCG-depressed mice in comparison to the control group (Fig. 4D, E). Moreover, the percentage of both Ly6G<sup>+</sup> and Ly6C<sup>+</sup> MDSCs was increased in the spleens of depressed BCG mice (Fig. 4F-H). These data indicate the increased immune suppressive Treg and monocytic MDSCs cells in depressed BCG mice that leads to lower vaccine efficacy.

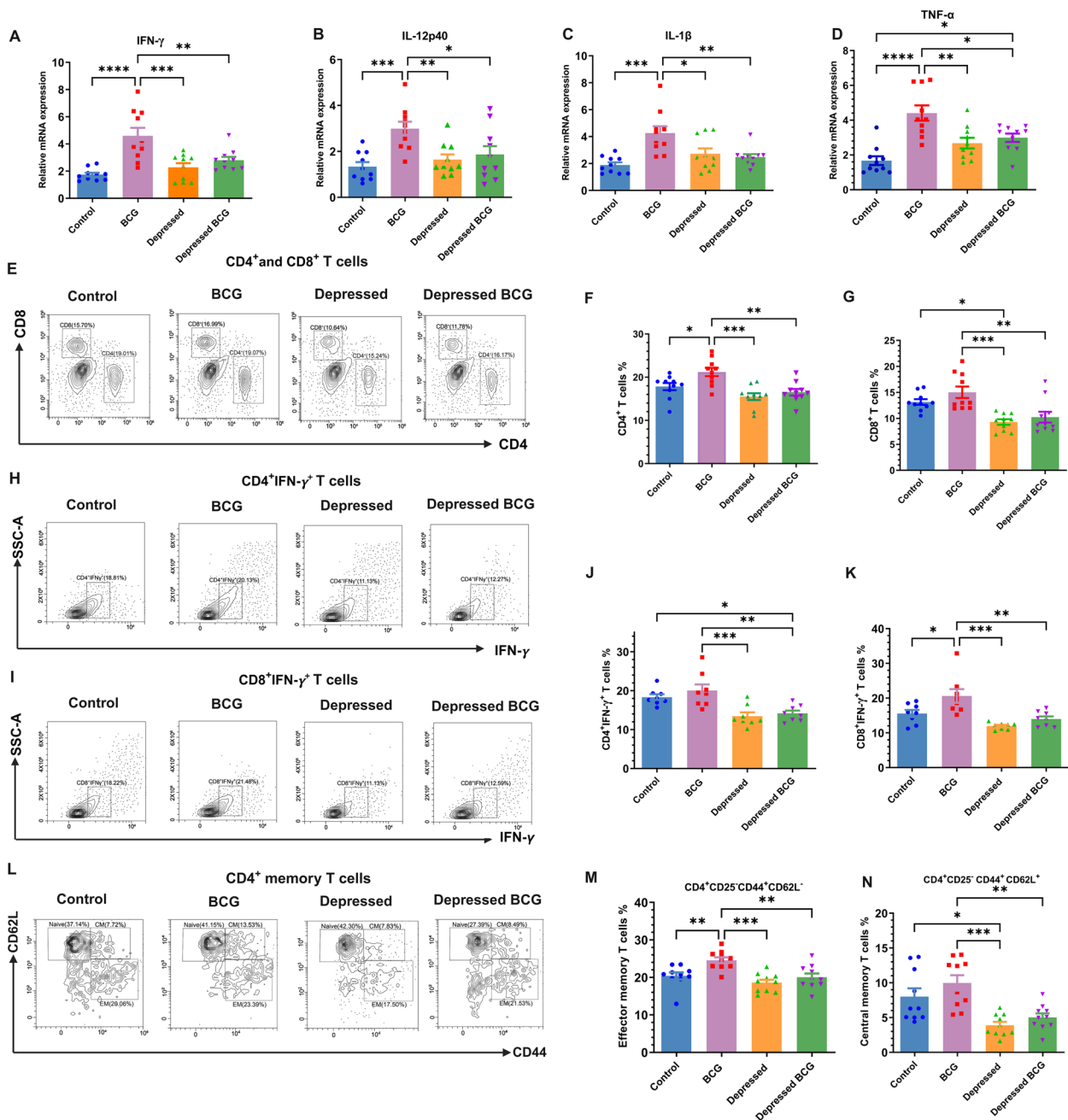


**Fig. 3** Evaluation of polyfunctional CD4<sup>+</sup>/CD8<sup>+</sup> T cells and depression effects on BCG immunomodulation. **A-D** The mRNA expression of IFN- $\gamma$ , IL12p40, IL1 $\beta$  and TNF- $\alpha$  cytokines was calculated in the spleen after euthanization in all four groups of mice. The significance is calculated compared with the control group. **E** Demonstrative gating of CD4<sup>+</sup> and CD8<sup>+</sup> cells of the indicated groups generated with CytExpert flow cytometry software. **F-G** Quantification of CD4<sup>+</sup> and CD8<sup>+</sup> frequencies in the spleens of all four groups of mice. **H-I** Gating images for phenotypic characterization of CD4<sup>+</sup>IFN $\gamma$ <sup>+</sup> and CD8<sup>+</sup>IFN $\gamma$ <sup>+</sup> T cells. **J-K** The percentage of IFN $\gamma$ <sup>+</sup> cells in both CD4<sup>+</sup> and CD8<sup>+</sup> T cells was analyzed and depicted for all four groups of mice. Their significance was evaluated by comparison with the control group. **L** Descriptive images for gating both CD4<sup>+</sup> central and effector memory immune cells. **M-N** Similarly, the relative percentage of CD4<sup>+</sup> cells, including the phenotype of effector memory (CD25<sup>-</sup>CD44<sup>+</sup>CD62L<sup>-</sup>) and central memory (CD25<sup>-</sup>CD44<sup>+</sup>CD62L<sup>+</sup>) T cells, in the spleens of all four groups of mice was determined. \*,  $p \leq 0.05$ ; \*\*,  $p \leq 0.01$ ; \*\*\*,  $p \leq 0.001$ ; \*\*\*\*,  $p \leq 0.0001$  (one-way ANOVA). Data are representative of three independent experiments with three biological replicates (mean  $\pm$  SEM)

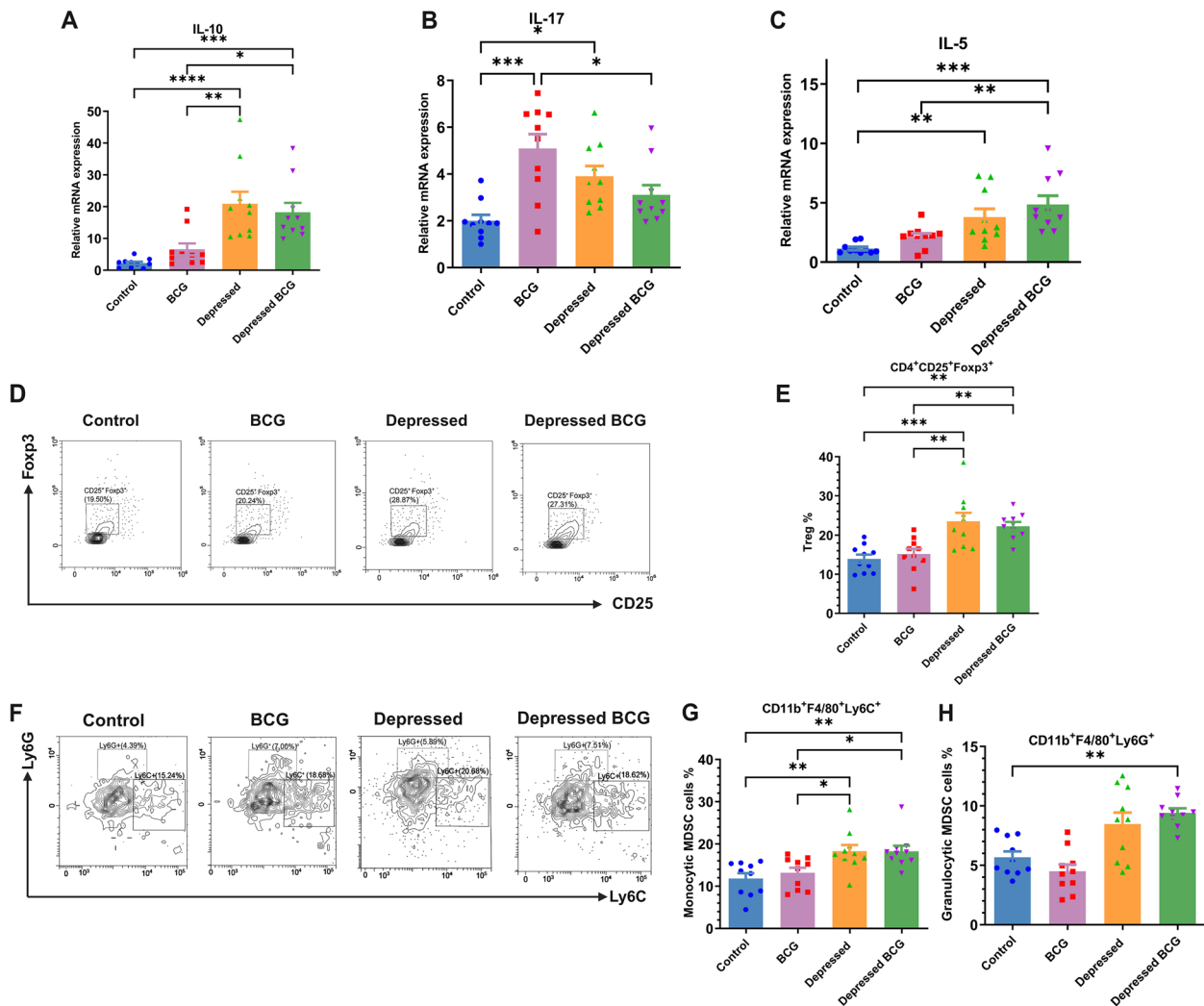


**Fig. 4** Understanding the BCG efficacy downfall mechanism in depressed mice. **A-C** mRNA expression of IL-10, IL-17 and IL-5 was quantified by qRT-PCR. **D** Gating of Treg cells. **E** The percentage of regulatory T cells was calculated for all four groups in comparison with the control group. **F** The CD11b<sup>+</sup> cells were segregated and gated according to the Ly6G<sup>+</sup> and Ly6G<sup>-</sup> antibodies depicted in the images. **G, H** The percentage of granulocytic-MDSCs (Ly6C<sup>-</sup>Ly6G<sup>+</sup>) and monocytic MDSCs (Ly6C<sup>+</sup>Ly6G<sup>-</sup>) found in splenocytes in different sets of mice. \*,  $p \leq 0.05$ ; \*\*,  $p \leq 0.01$ ; \*\*\*,  $p \leq 0.001$ ; \*\*\*\*,  $p \leq 0.0001$  (one-way ANOVA). Data are representative of three independent experiments with three biological replicates (mean  $\pm$  SEM)

## Discussion

The BCG antigenic response can control disseminated tuberculosis and tuberculosis meningitis, but it fails to prevent primary infection, reactivation, and pulmonary tuberculosis (Moliva et al. 2017). Hence, there is a need to understand the involvement of host cells and other factors that affect the induction of protective immunity countering *M. tuberculosis* and to utilize them to improve vaccine efficacy. Behavioral science and the immune system have many interlinked roles and affect each other's functions (Bains and Sharkey, 2022). In the current study,

we attempted to understand this crosstalk and its effect on vaccine responses in mice.

To induce depression in C57BL/6J mice, an assured depression model, chronic social defeat stress (CSDS), was established (Mancha-Gutierrez et al. 2021). By evaluating social interaction, forced swimming, the sucrose preference test and physiological changes in body weight, we quantified and qualified the susceptible mice (Serchov et al. 2016). To estimate any changes in immune homeostasis, a group of naïve control and depressed mice were studied simultaneously

without any vaccination (Bali et al 2015). After attaining depressed mice, we assessed the effector role of splenic T cells from naïve/immunized control and depressed mice using an MGIA assay (Parra et al. 2009; Pepponi. 2017). Strikingly, the clearance of phagocytosed bacteria by splenic effector T cells was significantly increased in depressed subjects. In this context, immunization with BCG also remains less effective. This indicated that depressive behavior in mice disrupts the efficiency of BCG vaccine immunity. Furthermore, the CFU load in the lungs and spleens of immunized depressed mice was high in comparison to the control mice (Kurtz et al. 2020). The organ index of both the lungs and spleen in depressed mice and depressed BCG mice improved below par, as it correlated with the decreasing total weight due to depression with a reduced inflammatory response.

We then observed that the fold-change of pro-inflammatory cytokines IFN- $\gamma$ , IL-12p40, IL-1 $\beta$  and TNF- $\alpha$  significantly declined in both the depressed and BCG-immunized depressed mice in comparison to their respective controls. These cytokines are reported to be important in generating trained immunity via the BCG immunomodulatory response (Cooper et al. 2011; Martinez-Penez et al. 2020).

Concurrently, the presence of antigen-specific IFN- $\gamma$  releasing T cells was significantly decreased in the depressed mice. This may be responsible for the failure of BCG and many other tuberculosis vaccinations or even affect their efficacy (Zhang et al. 2016). To understand the effects on adaptive immunity, which is much needed for effective vaccine response, we quantified the central and effector memory CD4<sup>+</sup> T cells, which were also lower in depressed subjects with/without BCG vaccination (Gunaseena et al. 2022).

We also observed escalation in the immune-suppressive cytokines IL-10 and IL-5 in depressed mice. IL-10 is increased multiple times in the spleen and antagonizes CD4<sup>+</sup> T-cell priming and effector cell activation, thus limiting T cell migration to the lungs and leading to limited infection control (Ferreira et al. 2021; Porro et al. 2020). Meanwhile, the decline in IL-17 in depressed mice lowers the induction of CXCR3 chemokine ligand 9, 10 and 11 (CXCL9-11), which recruits CD4<sup>+</sup>IFN- $\gamma$ <sup>+</sup> T cells (Chen et al. 2019) and CXCL13 to induce neutrophil migration to the infection site for the pathogen regulation (Tecchio and Cassatella, 2016).

We performed flow cytometry analysis to quantify immune-suppressive cells population, namely, MDSCs and Tregs, in the spleen of all four sets of mice (Gabrilovich and Nagaraj, 2009; Dikiy and Rudensky, 2023). We observed that both Tregs and MDSCs were present at a higher percentage in the spleens

of BCG-vaccinated depressed mice than in BCG mice (Hong et al. 2013). The roles of Tregs together with MDSCs are well understood in cancer biology and bacterial infection, but there is a lack of understanding about their role in vaccination (Lindau et al. 2013). It is known that an increase in both Ly6c<sup>+</sup> and Ly6g<sup>+</sup> MDSCs in the spleen of depressed mice can repress Natural killer cytotoxic cells in depressed subjects to affect vaccine efficacy in mice (Magcwebeba et al. 2019).

Thus, we can infer that Treg cells' elevated response due to depression affects the inflammatory response in mice, leading to a decrease in IFN- $\gamma$  producing T lymphocytes and memory T cells. Interestingly, it also mutually affects CD4<sup>+</sup> central and effector T memory cells in depressed subjects, retarding trained immunity by BCG vaccination. In the future, it would be important to check the role of epigenetic changes in depressed subjects contributing to the lowering of the immune response and quantify the effects on humoral immunity cells and antibody production. These data may facilitate the design of novel vaccines and immunotherapeutic interventions against pulmonary tuberculosis.

## Conclusion

Our study demonstrates that depression induces Tregs and MDSCs that perform an immunosuppressive function against the immune response generated by BCG.

## Methods

### Bacterial strains

*M. tuberculosis* H37Ra and *M. bovis* BCG were cultured at 37°C under static conditions in Middlebrook 7H9 broth (Becton Dickinson, New Jersey, USA, 271,310) supplemented with 10% oleic albumin dextrose catalase (OADC, Becton Dickinson, New Jersey, USA), 0.05% Tween 80, and 0.5% glycerol or on solid Middlebrook 7H11 agar plates (Becton Dickinson, New Jersey, USA) supplemented with 10% OADC and 0.5% glycerol. *M. tuberculosis* RFP-H37Ra was maintained by the addition of 50  $\mu$ g/mL hygromycin B.

For mouse immunization, BCG cultures were centrifuged at 3,000 $\times$ g for 10 min to pellet the bacteria. The pellet was resuspended in PBS to achieve 3 $\times$ 10<sup>6</sup> bacteria/ml and passed several times through an insulin syringe to disperse the bacteria.

For the mycobacterium growth inhibition assay (MGIA), the RFP-H37Ra culture optical density at OD<sub>600nm</sub> was adjusted to achieve the needed multiplicity of infection (MOI) and centrifuged at 3,000 $\times$ g for 10 min to pellet the bacteria. The pellet was resuspended in the infection medium and passed through an insulin syringe several times to disperse the bacteria.

To activate splenocytes into effector T cells, the H37Ra pellet was washed and suspended in PBS and then autoclaved at 121°C for 15 min, followed by filtration to remove precipitates to prepare whole-cell lysates.

### Animals

C57BL/6J mice (male, 6 weeks old) and retired breeder CD-1 mice (male, 4–6 months old) were obtained from the Laboratory Animal Center, Huazhong Agricultural University. After arrival, C57BL/6J mice were kept five per cage and habituated for 1 week, and CD-1 mice were kept in individual cages and acclimated for one week before being used in further experiments. The C57BL/6J mice were divided into four groups (control, BCG, depressed and depressed BCG groups), with 10 mice in each group. The control group was immunized with PBS on day 0 and not subjected to chronic social defeat stress (CSDS). The BCG group was immunized with BCG on day 0 and not subjected to CSDS. The depressed group was immunized with PBS on day 0 and subjected to CSDS. The depressed BCG group was immunized with BCG on day 0 and subjected to CSDS (Fig. 1A). The BCG response was evaluated 8 weeks after immunization.

### Immunization

Ten C57BL/6J male mice were immunized with BCG using an aerosol infection chamber (Bhaskar and Upadhyay, 2003). The mice were placed in a chamber that had been sterilized with alcohol and UV, the chamber was sealed, and the airflow was turned on. The chamber was saturated with PBS aerosol for 5 min and then BCG aerosol for 15 min to achieve 400–500 bacilli in the lungs of each mouse. For control mice, no BCG was added to the PBS (Schroeder et al. 2009).

### Chronic Social Defeat Stress (CSDS)

Non-experimental C57BL/6J mice were used as screeners to screen the CD-1 aggressor mice. The screening process was performed once daily for 3 successive days. A screener was put into the CD-1 resident cage for 3 min per session. On each subsequent day, we used different screening tools for each CD-1 mouse. An aggressor CD-1 mouse was selected for further CSDS experiments by the following criteria: (1) the initial aggression time had to be within 1 min of the beginning of the session, (2) pulling down and biting the screener for at least 5 s, and (3) the CD-1 mouse attacked a screener in at least two consecutive sessions.

CSDS was carried out as previously reported (Golden et al. 2011). Briefly, an aggressor CD-1 mouse was put on one part of the separated home cage during the night

before initiating the CSDS. On day 1, a C57BL/6J mouse was put into the compartment of the resident aggressor's home cage for 10 min. The intruder was transferred to the opposite compartment divided by an acrylic divider with holes at the end of time. One intruder was exposed to social defeat for 10 days and was moved daily to a new resident's home cage. Control mice were housed in similar compartmentalized cages and rotated to a new cage daily without physical contact with their cage members. The experiment was conducted between 3–5 p.m. Behavioral experiments were performed between 3–6 p.m. starting on day 11. We performed and analyzed behavior tests to find two groups of mice, namely, depressed and resilient mice, which were evaluated with comparison to the control group.

### SIT (Social Interaction Test)

SIT was performed as described (Golden et al. 2011; Kim et al. 2017) with some modifications. SIT consisted of two 3 min sessions, with a 30 s break. During the “no CD-1 target” session, there was an empty transparent plastic cage. In the “CD-1 target” session, a CD-1 aggressor mouse was put into the transparent plastic cage. The CD-1 aggressor is novel to the defeated C57BL/6J mouse. The movement of the test C57BL/6J mouse was recorded using a tracking system (Smart Video Tracking Software—PANLAB) in an open field, uniform size Plexiglas box (40 L × 40 W × 40 H cm). The cumulative time of the movement in the “interaction zone” and the “corner zone” were calculated. The SI ratio was calculated as follows: SI ratio (%) = interaction zone time of “target” trial / interaction zone time of “no target” trial × 100 (Robie et al. 2017). Mice showing less than a 100% SI ratio were regarded as depressed mice. Mice showing an SI ratio above 100% belong to the resilient group, which did not proceed with further immunological studies (Krishnan et al. 2007).

### Forced Swimming Test (FST)

We used an FST protocol previously used (Porsolt et al. 2001). Briefly, each mouse was placed into a clear plastic cylinder (16 cm diameter × 28 cm height) filled with fresh 15–18 cm of water at 23–26°C for 6 min. Immobility time (IT) was measured using a system (Smart Video Tracking Software—PANLAB) during the last 4 min of the test. The condition for immobility or passive swimming was floating vertically in the water while making only those fundamental movements to maintain the head above the water. Mice were dried and normally housed after the test.

### Sucrose Preference Test (SPT)

After the FST, all C57BL/6J mice underwent the SPT to estimate a reduced preference for the sweet solution. The mice were separated single per cage and presented to two drinking bottles: one containing 1% sucrose and the other water for 4 days in their home cage with positions of fluids switched daily. The percentage of the volume of sucrose intake over the total volume of fluid intake and averaged over the four days of testing was calculated as follows: sucrose preference =  $V(\text{sucrose solution}) / [V(\text{sucrose solution}) + V] \times 100\%$  (Serchov et al. 2016).

### Colony-Forming Unit (CFU) assay

Homogenates of both the spleen and lung were taken after serial dilution of 1/10 times in PBS from the BCG-infected groups. Then, 100  $\mu\text{l}$  was spread onto Middlebrook 7H11 agar containing OADC enrichment Petri plates containing PENTA antibiotics (BBL MGIT, Becton, Dickinson) incubated at 37°C for approximately three weeks for bacterial CFU counting. All experiments were performed in triplicate, and colonies were counted manually.

### Hematoxylin and Eosin (H&E) staining

Part of the lungs was obtained from the control, BCG, depressed and depressed BCG mice and was fixed with 4% paraformaldehyde for 24 h. Then, the tissue was embedded in parafilm for H&E staining. Paraffin sections of 5  $\mu\text{m}$  thickness were cut, and sections were stained with hematoxylin and eosin. All alveolar tissue health was determined by investigating the tissue under a compound microscope.

### In vitro Mycobacterial Growth Inhibition Assay (MGIA)

The MGIA for evaluating the BCG vaccine was based on procedures described earlier (Parra et al. 2009). Bone marrow-derived macrophages (BMDMs) were prepared by flushing the femurs of mice with complete Dulbecco's modified Eagle's medium (DMEM) supplemented with 10% fetal bovine serum (FBS) and 20 ng/mL macrophage colony stimulating factor (MCSF). BMDM ( $7 \times 10^5$ ) were plated in a 24-well plate for 7 days to obtain a confluent monolayer at 37°C in 5%  $\text{CO}_2$ . *M. tuberculosis* RFP-H37Ra (MOI = 10) was added to each well for 12 h and then washed three times with PBS to remove extracellular bacteria. The cells were incubated with DMEM at 37°C in 5%  $\text{CO}_2$  for 48 h to obtain target BMDMs.

H37Ra lysate-activated splenocytes were used as effector T cells to determine the efficacy of the BCG vaccine against mycobacteria localized inside the target BMDMs.

**Table 1** qRT-PCR Primers

Name	Seq. (5'-3')
IFN- $\gamma$ For	TTCTTCAGCAACAGCAAGGC
IFN- $\gamma$ Rev	TCAGCAGCGACTCCTTTTCC
IL-17 For	TCTCCACCGCAATGAAGACC
IL-17 Rev	CACACCCACCAGCATCTTCT
IL-10 For	ATAACTGCACCCACTTCCCA
IL-10 Rev	GGGCATCACTTCTACCAGGT
TNF- $\alpha$ For	ATGAGACAGAAAGCATGAT
TNF- $\alpha$ Rev	AGTAGACAGAAGAGCGTGGT
IL-1 $\beta$ For	CCTCTGATGGCAACCCTT
IL-1- $\beta$ Rev	TTCATCCCCCACAGTTGAC
IL-12p40 For	GATGACATGGTGAAGACGGC
IL-12p40 Rev	AGGCACAGGGTCATCATCAA
IL-5 For	ACCGAGCTCTGTTGACAAG
IL-5 Rev	TCCTCGCCACACTTCTTTT
$\beta$ -actin For	CGCCACCAAGTTCGCCATGGA
$\beta$ -actin Rev	TACAGCCCGGGAGCATCGT

**Table 2** Antibodies for flow cytometry

Cell type	Gating strategy
IFN $\gamma$ producing CD4 T cells	CD4 <sup>+</sup> IFN $\gamma$ <sup>+</sup>
IFN $\gamma$ producing CD8 T cells	CD8 <sup>+</sup> IFN $\gamma$ <sup>+</sup>
Naïve memory T cells	CD4 <sup>+</sup> CD25 <sup>-</sup> CD62L <sup>+</sup> CD44 <sup>-</sup>
Tregs	CD4 <sup>+</sup> CD25 <sup>+</sup> Foxp3 <sup>+</sup>
MDSC Ly6C <sup>+</sup>	F4/80 <sup>+</sup> CD11b <sup>+</sup> Ly6G <sup>-</sup> Ly6C <sup>+</sup>
MDSC Ly6G <sup>+</sup>	F4/80 <sup>+</sup> CD11b <sup>+</sup> Ly6G <sup>+</sup> Ly6C <sup>-</sup>
Central memory T cells	CD4 <sup>+</sup> CD25 <sup>-</sup> CD62L <sup>+</sup> CD44 <sup>+</sup>
Effector memory T cells	CD4 <sup>+</sup> CD25 <sup>-</sup> CD62L <sup>-</sup> CD44 <sup>+</sup>

According to the previously discussed method (Kolibab et al. 2009), spleens from control, BCG, depressed, and depressed BCG mice were ruptured by a pair of frosted glass slides to obtain a clear single cell suspension. After RBC lysis with red cell lysis buffer (Biosharp, BL503) for 5 min at RT, the cells were pelleted at 1500 g and resuspended in PBS (ice cold). The adherent splenic macrophages were removed by allowing them to adhere to flasks for 30 min incubation at 37°C and gently pipetting the suspension to recover the nonadherent cells. After a PBS wash, the viability was assessed by segregation of trypan blue. T cells were expanded with mycobacterium antigen for seven days to obtain effector T cells. A total of  $3 \times 10^6$  effector T cells were applied to  $7 \times 10^5$  target BMDM cells and incubated for 48 h. Then, the macrophages were lysed with 0.2% saponin for 2–3 min at RT. The lysate dilutions were plated onto 7H11 plates for colony counting.

### Quantitative real-time PCR (qRT-PCR)

The mouse spleen cell suspension was activated in the presence of 20 µg/mL of *M. tuberculosis* whole cell lysate for 6 h. Total RNA was extracted by using RNA<sup>iso</sup> Plus reagent (TAKARA) according to the manufacturer's instructions. cDNA was prepared from 1 µg RNA using the ReverTra Ace qPCR RT Master Mix kit (Toyobo LifeScience, Shanghai, China). Relative gene expression was obtained by quantitative real-time PCR (VIA7System, Thermo Fisher) with SYBR Green Mix (Thermo Fisher) using specific cytokine primers, as shown in Table 1. Expression of the specific genes was normalized using  $\beta$ -actin (mouse) mRNA levels as an internal control.

### Flow cytometry

Red blood cells (RBCs) were lysed using red cell lysis solution (Biosharp, BL503). Cells were resuspended in staining buffer (PBS containing 1% fetal bovine serum (FBS) and 0.05% sodium azide). A total of  $3 \times 10^6$  cells were incubated with antibody mix at 4 °C for 30 min, after which the cells were washed three times with PBS. The cells were resuspended in PBS containing 1% FBS. Antibodies used for staining included FITC rat anti-mouse CD4 (1:250, 553046, BD Biosciences), APC rat anti-mouse CD8a (1:250, 553035, BD Biosciences), PerCP-Cy5.5 rat anti-mouse CD44 (1:150, 560570, BD Biosciences), PE-Cy7 rat anti-mouse CD62L (1:200, 560516, BD Biosciences), PE rat anti-mouse IFN- $\gamma$  (1:250, 554412, BD Biosciences), APC-H7 rat anti-mouse Ly-6G (1:150, 565369, BD Biosciences), V450 rat anti-mouse Foxp3 (1:100, 561293, BD Biosciences), APC-Cy7 rat anti-mouse CD25 (1:250, 561038, BD Biosciences), FITC rat anti-mouse Ly-6C (1:150, 561085, BD Biosciences), PE rat anti-mouse CD11b (1:250, 101207, BioLegend), and V-450 rat anti-mouse F4/80 (1:200, 101207, BioLegend). We used a flow cytometer (Beckman CytoFLEX LX, USA) to conduct our experiments, and the data were analyzed using CytExpert software. For intracellular staining, a BD Cytofix/Cytoperm™ Fix/Perm Kit (Cat. No. 554714) was used, and staining was performed according to the manufacturer's instructions. A panel of gating specific cell types is depicted in Table 2.

### Statistical analysis

All experimental data were plotted using GraphPad Prism 9.0 (La Jolla, CA, USA) as analytical software and are presented as the mean  $\pm$  SEM. Assessment of the significant difference among different sets was executed by using two-way/one-way ANOVA or Student's *t* test. Significant differences in the data are shown as \*, \*\*, \*\*\* and \*\*\*\* when *p* values  $\leq 0.05$ ,  $\leq 0.01$ ,  $\leq 0.001$ , and  $\leq 0.0001$ , respectively.

### Abbreviations

<i>M. tuberculosis</i>	<i>Mycobacterium tuberculosis</i>
BCG	Bacillus Calmette-Guérin
CFU	Colony-forming units
MGIA	Mycobacterial Growth Inhibition Assay
BMDMs	Bone marrow-derived macrophages
CSDS	Chronic Social Defeat Stress
MDSC	Myeloid-derived suppressor cells
Ly6C	Lymphocyte antigen 6 complex, locus C1
Ly6G	Lymphocyte antigen 6 complex locus G6D
IFN- $\gamma$	Interferon- $\gamma$
Th cells	T helper cells
IL-1 $\beta$	Interleukin-1 $\beta$
IL-12p40	Interleukin-12p40
IL-10	Interleukin-10
IL-17	Interleukin-17
IL-5	Interleukin-5
TNF- $\alpha$	Tumor necrosis factor- $\alpha$
CD8	Cluster of differentiation 8
CD4	Cluster of differentiation 4
Tregs	Regulatory T cells

### Supplementary Information

The online version contains supplementary material available at <https://doi.org/10.1186/s44149-023-00102-x>.

**Additional file 1: Supplementary Fig. 1.** Gating strategy of different parameters using flow cytometry. (A) Gating of IFN $\gamma$ -positive CD4<sup>+</sup> and CD8<sup>+</sup> T cells. (B) Gating of CD4<sup>+</sup> and CD8<sup>+</sup> memory T cells. (C) Gating of CD4<sup>+</sup> regulatory T cells. (D) Gating of Distinct Myeloid-derived suppressor cells (MDSCs)-Monocytic-MDSCs (Ly6C<sup>+</sup>Ly6G<sup>-</sup>) and Granulocytic-MDSCs (Ly6C<sup>-</sup>Ly6G<sup>+</sup>).

**Additional file 2: Supplementary Fig. 2.** CD8<sup>+</sup> memory T cells show less significance in depressed mice. (A) Gating of CD8<sup>+</sup> memory T cells in all indicated groups of mice. (B-C) CD8<sup>+</sup> effector and central cell percentages evaluated from total splenocytes in all four groups of mice. \*, *p*  $\leq 0.05$ ; \*\*, *p*  $\leq 0.01$ ; \*\*\*, *p*  $\leq 0.001$ ; \*\*\*\*, *p*  $\leq 0.0001$  (one-way ANOVA). Data are representative of three independent experiments with three biological replicates (mean  $\pm$  SEM).

### Acknowledgements

We would like to thank the National Key Laboratory of Agricultural Microbiology Core Facility for assistance in flow cytometry and qRT-PCR, and we would be grateful to Dr. Fangkui Wang for his support of data acquisition and analysis.

### Authors' contributions

G. C and R.T contributed to the conception and design of this study. R.T executed the experiments and analyzed the data. R.T and Y. L wrote the first draft of the manuscript. X.C edited the manuscript. R.T. and A.D. performed flow cytometry analysis. B.Y. and Z.W. performed the review of the final manuscript. G.C. arranged the funding for the study. A.R. helped visualize the h and e pictures. All the authors discussed the results and commented on the document.

### Funding

This study was funded by the National Natural Science Foundation of China (Grant No. U21A20259, 31602061, 31872470) and the National Key Research and Development Program of China (Grant No. 2021YFD1800401).

### Availability of data and materials

Relevant data and material in this article are available and can be requested from the corresponding authors.

### Declarations

#### Ethics approval and consent to participate

The animal experiments were approved by the Scientific Ethics Committee of Huazhong Agricultural University (HZAUMO-2019-105).

**Consent for publication**

Not applicable.

**Competing interests**

All contributing authors declare no competing interests. Author Gang Cao was not involved in the journal's review or decisions related to this manuscript.

Received: 30 August 2023 Accepted: 9 October 2023

Published online: 18 December 2023

**References**

- Abubakar, I., L. Pimpin, C. Ariti, R. Beynon, P. Mangtani, J.A.C. Sterne, P.E.M. Fine, et al. 2013. Systematic review and meta-analysis of the current evidence on the duration of protection by bacillus calmette-guérin vaccination against *Tuberculosis*. *Health Technology Assessment (Winchester, England)* 17 (37): 1. <https://doi.org/10.3310/hta17370>.
- Bagcchi, S. 2023. Who's global *Tuberculosis* report 2022. *The Lancet Microbe* 4 (1): e20. [https://doi.org/10.1016/S2666-5247\(22\)00359-7](https://doi.org/10.1016/S2666-5247(22)00359-7).
- Bains, N., and S. Abdijadid. 2023. Major Depressive Disorder. StatPearls publishing.
- Bains, J.S., and K.A. Sharkey. 2022. Stress and immunity — the circuit makes the difference. *Nature Immunology* 23 (8): 1137–39. <https://doi.org/10.1038/s41590-022-01276-1>.
- Bali, P., S. Tousif, G. Das, and L. Van Kaer. 2015. Strategies to improve BCG vaccine efficacy. *Immunotherapy* 7 (9): 945–48. <https://doi.org/10.2217/imt.15.60>.
- Bhaskar, S., and U. Pramod. 2003. Design and evaluation of an aerosol infection chamber for small animals. *International Journal of Pharmaceutics* 255 (1–2): 43–48. [https://doi.org/10.1016/S0378-5173\(03\)00023-1.kilindau](https://doi.org/10.1016/S0378-5173(03)00023-1.kilindau).
- Buddle, B.M., D. Shu, N.A. Parlane, S. Subharat, A. Heiser, R.G. Hewinson, H.M. Vordermeier, and D.N. Wedlock. 2016. Vaccination of cattle with a high dose of BCG vaccine 3 weeks after experimental infection with mycobacterium bovis increased the inflammatory response, but not tuberculous pathology. *Tuberculosis (Edinb)* 99: 120–27. <https://doi.org/10.1016/j.tube.2016.05.004>.
- Chen, J., X. Ye, E. Pitmon, M. Lu, J. Wan, E.R. Jellison, A.J. Adler, A.T. Vella, and K. Wang. 2019. IL-17 Inhibits Cxcl9/10-Mediated Recruitment of Cd8(+) Cytotoxic T Cells and Regulatory T Cells to Colorectal Tumors. *Journal for Immunotherapy of Cancer* 7 (1): 324. <https://doi.org/10.1186/s40425-019-0757-z>.
- Cooper, A.M., Mayer-Barber, D. Katrin, and A. Sher. 2011. Role of Innate Cytokines in Mycobacterial Infection. *Mucosal Immunology* 4 (3): 252–60. <https://doi.org/10.1038/mi.2011.13>.
- Dikiy, S., and A.Y. Rudensky. 2023. Principles of Regulatory T-Cell Function. *Immunity* 56 (2): 240–55. <https://doi.org/10.1016/j.immuni.2023.01.004>.
- Ferreira, C.M., A.M. Barbosa, P. Barreira-Silva, R. Silvestre, C. Cunha, A. Carvalho, F. Rodrigues, et al. 2021. Early IL-10 Promotes Vasculature-Associated Cd4+ T Cells Unable to Control Mycobacterium Tuberculosis Infection. *JCI Insight* 6 (21). <https://doi.org/10.1172/jci.insight.150060>.
- Gabrilovich, D.I., and S. Nagaraj. 2009. Myeloid-Derived Suppressor Cells as Regulators of the Immune System. *Nature Reviews Immunology* 9 (3): 162–74. <https://doi.org/10.1038/nri2506>.
- Golden, S.A., H.E. Covington III, O. Berton, and S.J. Russo. 2011. A Standardized Protocol for Repeated Social Defeat Stress in Mice. *Nature Protocols* 6 (8): 1183–91. <https://doi.org/10.1038/nprot.2011.361>.
- Gong, Q.L., Y. Chen, T. Tian, X. Wen, D. Li, Y.H. Song, Q. Wang, D. Rui, and X.X. Zhang. 2021. Prevalence of Bovine Tuberculosis in Dairy Cattle in China During 2010–2019: A Systematic Review and Meta-Analysis. *PLoS Neglected Tropical Diseases* 15 (6): e0009502. <https://doi.org/10.1371/journal.pntd.0009502>.
- Gunasena, M., R.K. Shukla, N. Yao, O.R. Mejia, M.D. Powell, K.J. Oestreich, M. de Jesús. Aceves-Sánchez, et al. 2022. Evaluation of Early Innate and Adaptive Immune Responses to the Tb Vaccine Mycobacterium Bovis BCG and Vaccine Candidate BCGΔBCG1419c. *Scientific Reports* 12 (1): 12377. <https://doi.org/10.1038/s41598-022-14935-y>.
- Hales, Claire A., Sarah A. Stuart, Michael H. Anderson, and Emma S.J. Robinson. 2014. Modeling Cognitive Affective Biases in Major Depressive Disorder Using Rodents. *British Journal of Pharmacology* 171 (20): 4524–38. <https://doi.org/10.1111/bph.12603>.
- Henao-Tamayo, Marcela I., Diane J. Ordway, Scott M. Irwin, Shaobin Shang, Crystal Shanley, and Ian M. Orme. 2010. Phenotypic Definition of Effector and Memory T-Lymphocyte Subsets in Mice Chronically Infected with Mycobacterium Tuberculosis. *Clinical and Vaccine Immunology* 17 (4): 618–25. <https://doi.org/10.1128/cvi.00368-09>.
- Hong, M., J. Zheng, Z.Y. Ding, J.H. Chen, L. Yu, Y. Niu, Y.Q. Hua, and L.L. Wang. 2013. Imbalance between Th17 and Treg Cells May Play an Important Role in the Development of Chronic Unpredictable Mild Stress-Induced Depression in Mice. *Neuroimmunomodulation* 20 (1): 39–50. <https://doi.org/10.1159/000343100>.
- Khan, M.K., M.N. Islam, J. Ferdous, and M.M. Alam. 2019. An Overview on Epidemiology of Tuberculosis. *Mymensingh Medical Journal* 28 (1): 259–66.
- Kim, H.D., T. Call, S. Carotenuto, R. Johnson, and D. Ferguson. 2017. Testing Depression in Mice: A Chronic Social Defeat Stress Model. *Bioprotocol* 7 (7): e2203–e2303. <https://doi.org/10.21769/bioprotoc.2203>.
- Kolibab, K., M. Parra, A.L. Yang, L.P. Perera, S.C. Derrick, and S.L. Morris. 2009. A Practical *In Vitro* Growth Inhibition Assay for the Evaluation of Tb Vaccines. *Vaccine* 28 (2): 317–22. <https://doi.org/10.1016/j.vaccine.2009.10.047>.
- Krishnan, V., M.H. Han, D.L. Graham, O. Berton, W. Renthal, S.J. Russo, Q. Laplant, et al. 2007. Molecular Adaptations Underlying Susceptibility and Resistance to Social Defeat in Brain Reward Regions. *Cell* 131 (2): 391–404. <https://doi.org/10.1016/j.cell.2007.09.018>.
- Kurtz, S.L., A.P. Rossi, G.L. Beamer, D.M. Gatti, I. Kramnik, and K.L. Elkins. 2020. The Diversity Outbred Mouse Population Is an Improved Animal Model of Vaccination against Tuberculosis That Reflects Heterogeneity of Protection. *MSphere* 5 (2). <https://doi.org/10.1128/msphere.00097-20>.
- Lindau, Dennis, Paul Gielen, Michiel Kroesen, Pieter Wesseling, and J. Gosse. 2013. The Immunosuppressive Tumor Network: Myeloid-Derived Suppressor Cells, Regulatory T Cells and Natural Killer T Cells. *Immunology Adema* 138 (2): 105–15. <https://doi.org/10.1111/imm.12036>.
- Magcwebeba, T., A. Dorhoi, and N. du Plessis. 2019. The Emerging Role of Myeloid-Derived Suppressor Cells in Tuberculosis. *Frontiers in Immunology* 10: 917. <https://doi.org/10.3389/fimmu.2019.00917>.
- Mancha-Gutiérrez, H.M., E. Estrada-Camarena, L. Mayagoitia-Navales, E. López-Pacheco, and C. López-Rubalcava. 2021. Chronic Social Defeat During Adolescence Induces Short- and Long-Term Behavioral and Neuroendocrine Effects in Male Swiss-Webster Mice. *Frontiers in Behavioral Neuroscience* 15: 734054. <https://doi.org/10.3389/fnbeh.2021.734054>.
- Martínez-Pérez, A., A. Igea, O. Estévez, C.M. Ferreira, E. Torrado, A.G. Castro, C. Fernández, et al. 2020. Changes in the Immune Phenotype and Gene Expression Profile Driven by a Novel Tuberculosis Nanovaccine: Short and Long-Term Post-Immunization. *Frontiers in Immunology* 11: 589863. <https://doi.org/10.3389/fimmu.2020.589863>.
- Moliva, Juan I., Joanne Turner, and Jordi B. Torrelles. 2017. Immune Responses to Bacillus Calmette–Guérin Vaccination: Why Do They Fail to Protect against Mycobacterium Tuberculosis? *Frontiers in Immunology* 8: 407. <https://doi.org/10.3389/fimmu.2017.00407>.
- Parra, M., A.L. Yang, J. Lim, K. Kolibab, S. Derrick, N. Cadieux, L.P. Perera, et al. 2009. Development of a Murine Mycobacterial Growth Inhibition Assay for Evaluating Vaccines against Mycobacterium Tuberculosis. *Clinical and Vaccine Immunology* 16 (7): 1025–32. <https://doi.org/10.1128/cvi.00067-09>.
- Pepponi, I., B. Khatri, R. Tanner, B. Villarreal-Ramos, M. Vordermeier, and H. McShane. 2017. A Mycobacterial Growth Inhibition Assay (Mgia) for Bovine Tb Vaccine Development. *Tuberculosis* 106: 118–122. <https://doi.org/10.1016/j.tube.2017.07.008>.
- Porro, C., A. Cianciulli, and M.A. Panaro. 2020. The Regulatory Role of IL-10 in Neurodegenerative Diseases. *Biomolecules* 10 (7). <https://doi.org/10.3390/biom10071017>.
- Porsolt, R.D., G. Brossard, C. Hautbois, and S. Roux. 2001. Rodent Models of Depression: Forced Swimming and Tail Suspension Behavioral Despair Tests in Rats and Mice. *Current Protocols in Neuroscience* 14 (1): 8.10 A. 1–8.10 A. 10. <https://doi.org/10.1002/0471142301.ns0810as14>.
- Robie, A.A., K.M. Seagraves, S.E.R. Egnor, and K. Branson. 2017. Machine Vision Methods for Analyzing Social Interactions. *Journal of Experimental Biology* 220 (1): 25–34. <https://doi.org/10.1242/jeb.142281>.

- Romha, G., G. Gebru, A. Asefa, and G. Mamo. 2018. Epidemiology of Mycobacterium Bovis and Mycobacterium Tuberculosis in Animals: Transmission Dynamics and Control Challenges of Zoonotic Tb in Ethiopia. *Preventive Veterinary Medicine* 158: 1–17. <https://doi.org/10.1016/j.prevetmed.2018.06.012>.
- Roy A., M. Eisenhut, R.J. Harris, L.C. Rodrigues, Saranya Sridhar, Stephanie Habermann, Luke Snell, et al. 2014. Effect of BCG Vaccination against Mycobacterium Tuberculosis Infection in Children: Systematic Review and Meta-Analysis. *BMJ* 349. <https://doi.org/10.1136/bmj.g4643>.
- Schroeder, W.G., L.M. Mitrescu, M.L. Hart, R. Unnithan, J.M. Gilchrist, E.E. Smith, C. Shanley, et al. 2009. Flexible Low-Cost System for Small Animal Aerosol Inhalation Exposure to Drugs, Proteins, Inflammatory Agents, and Infectious Agents. *Biotechniques* 46 (3): Piii–Pviii. <https://doi.org/10.2144/000112895>.
- Seiler, A., C.P. Fagundes, and L.M. Christian. 2020. The Impact of Everyday Stressors on the Immune System and Health. In *Stress Challenges and Immunity in Space: From Mechanisms to Monitoring and Preventive Strategies*, ed. Alexander Choukèr, 71–92. Cham: Springer International Publishing. [https://doi.org/10.1007/978-3-030-16996-1\\_6](https://doi.org/10.1007/978-3-030-16996-1_6).
- Serchov, T., D. van Calker, and K. Biber. 2016. Sucrose Preference Test to Measure Anhedonic Behavior in Mice. *Bioprotocol* 6 (19): e1958–e58. <https://doi.org/10.21769/bioprotoc.1958>.
- Simmons, J.D., C.M. Stein, C. Seshadri, M. Campo, G. Alter, S. Fortune, E. Schurr, et al. 2018. Immunological Mechanisms of Human Resistance to Persistent Mycobacterium Tuberculosis Infection. *Nature Reviews Immunology* 18 (9): 575–89. <https://doi.org/10.1038/s41577-018-0025-3>.
- Singh, A.K., and U.D. Gupta. 2018. Animal Models of Tuberculosis: Lesson Learnt. *The Indian Journal of Medical Research* 147 (5): 456–63. [https://doi.org/10.4103/ijmr.ijmr\\_554\\_18](https://doi.org/10.4103/ijmr.ijmr_554_18).
- Tecchio, C., and M.A. Cassatella. 2016. Neutrophil-Derived Chemokines on the Road to Immunity. *Seminars in Immunology* 28 (2): 119–28. <https://doi.org/10.1016/j.smim.2016.04.003>.
- Waters, R.C., and E. Gould. 2022. Early Life Adversity and Neuropsychiatric Disease: Differential Outcomes and Translational Relevance of Rodent Models. *Frontiers in Systems Neuroscience* 16. <https://doi.org/10.3389/fnsys.2022.860847>.
- Williams, G.A., E. Scott-Baird, A. Núñez, F.J. Salguero, E. Wood, S. Houghton, and H.M. Vordermeier. 2022. The Safety of BCG Vaccination in Cattle: Results from Good Laboratory Practice Safety Studies in Calves and Lactating Cows. *Heliyon* 8 (12): e12356. <https://doi.org/10.1016/j.heliyon.2022.e12356>.
- Yang, J.D., D. Mott, R. Sutiwisesak, Y.J. Lu, F. Raso, B. Stowell, G.H. Babunovic, et al. 2018. Mycobacterium Tuberculosis-Specific Cd4+ and Cd8+ T Cells Differ in Their Capacity to Recognize Infected Macrophages. *PLoS Pathogens* 14 (5): e1007060. <https://doi.org/10.1371/journal.ppat.1007060>.
- Zhang, L., H.W. Ru, F.Z. Chen, C.Y. Jin, R.F. Sun, X.Y. Fan, M. Guo, et al. 2016. Variable Virulence and Efficacy of BCG Vaccine Strains in Mice and Correlation with Genome Polymorphisms. *Molecular Therapy* 24 (2): 398–405. <https://doi.org/10.1038/mt.2015.216>.
- Zhang, H., M. Liu, W. Fan, S. Sun, and X. Fan. 2022. The Impact of Mycobacterium Tuberculosis Complex in the Environment on One Health Approach. *Frontiers in Public Health* 10: 994745. <https://doi.org/10.3389/fpubh.2022.994745>.

## Publisher's Note

Springer Nature remains neutral with regard to jurisdictional claims in published maps and institutional affiliations.

Ready to submit your research? Choose BMC and benefit from:

- fast, convenient online submission
- thorough peer review by experienced researchers in your field
- rapid publication on acceptance
- support for research data, including large and complex data types
- gold Open Access which fosters wider collaboration and increased citations
- maximum visibility for your research: over 100M website views per year

At BMC, research is always in progress.

Learn more [biomedcentral.com/submissions](https://biomedcentral.com/submissions)

